nature energy

SUPPLEMENTARY INFORMATION

https://doi.org/10.1038/s41560-017-0054-3

In the format provided by the authors and unedited.

Large guanidinium cation mixed with methylammonium in lead iodide perovskites for 19% efficient solar cells

Alexander D. Jodlowski[1,2], Cristina Roldán-Carmona[1]*, Giulia Grancini[1], Manuel Salado[1,3], Maryline Ralaiarisoa[4,5], Shahzada Ahmad[3], Norbert Koch[4,5], Luis Camacho[2], Gustavo de Miguel[2]* and Mohammad Khaja Nazeeruddin[1]*

[1]Group for Molecular Engineering of Functional Materials, Institute of Chemical Sciences and Engineering, Ecole Polytechnique Fédérale de Lausanne (EPFL), Sion, Switzerland. [2]Departamento de Química Física y Termodinámica Aplicada, Instituto Universitario de Investigación en Química Fina y Nanoquímica IUQFN, Universidad de Córdoba, Campus de Rabanales, Edificio Marie Curie, Córdoba, Spain. [3]Abengoa Research, Abengoa, C/ Energía Solar no. 1, Campus Palmas Altas, Sevilla, Spain. [4]Humboldt-Universität zu Berlin, Institut für Physik & IRIS Adlershof, Berlin, Germany. [5]Helmholtz-Zentrum Berlin für Materialien und Energie, Devision Renewable Energies, Berlin, Germany. *e-mail: cristina.roldancarmona@epfl.ch; gmiguel@uco.es; mdkhaja.nazeeruddin@epfl.ch

Supplementary Figures

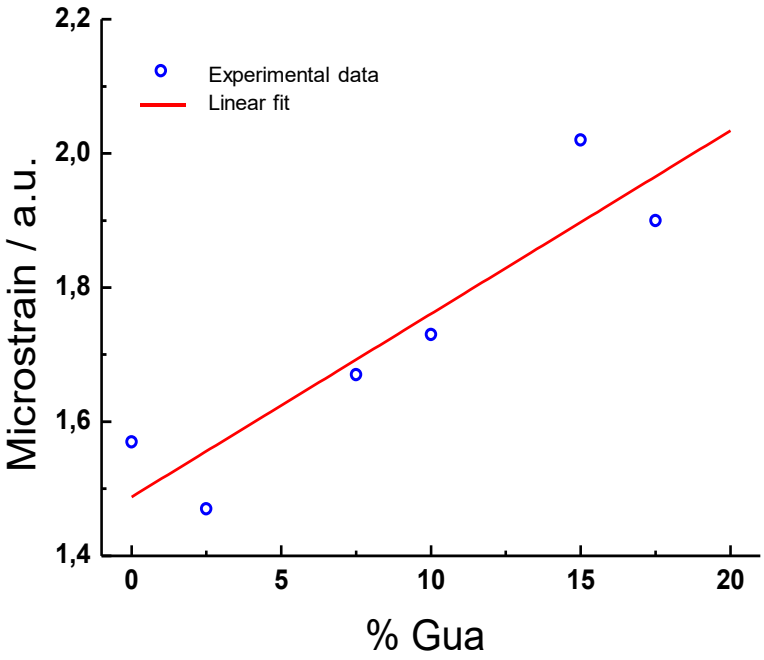

Supplementary Figure 1. Micro-strain (ε) variations in $MAPbI_3$ structure upon increasing Gua content. The ε values are estimated by using the Williamson-Hall equation, $\beta = {}^{1}/_{D} + {}^{2\varepsilon}/_{d}$, where β is the width of the reflection peaks, D is the crystallite size and d is the position of the reflections peaks.

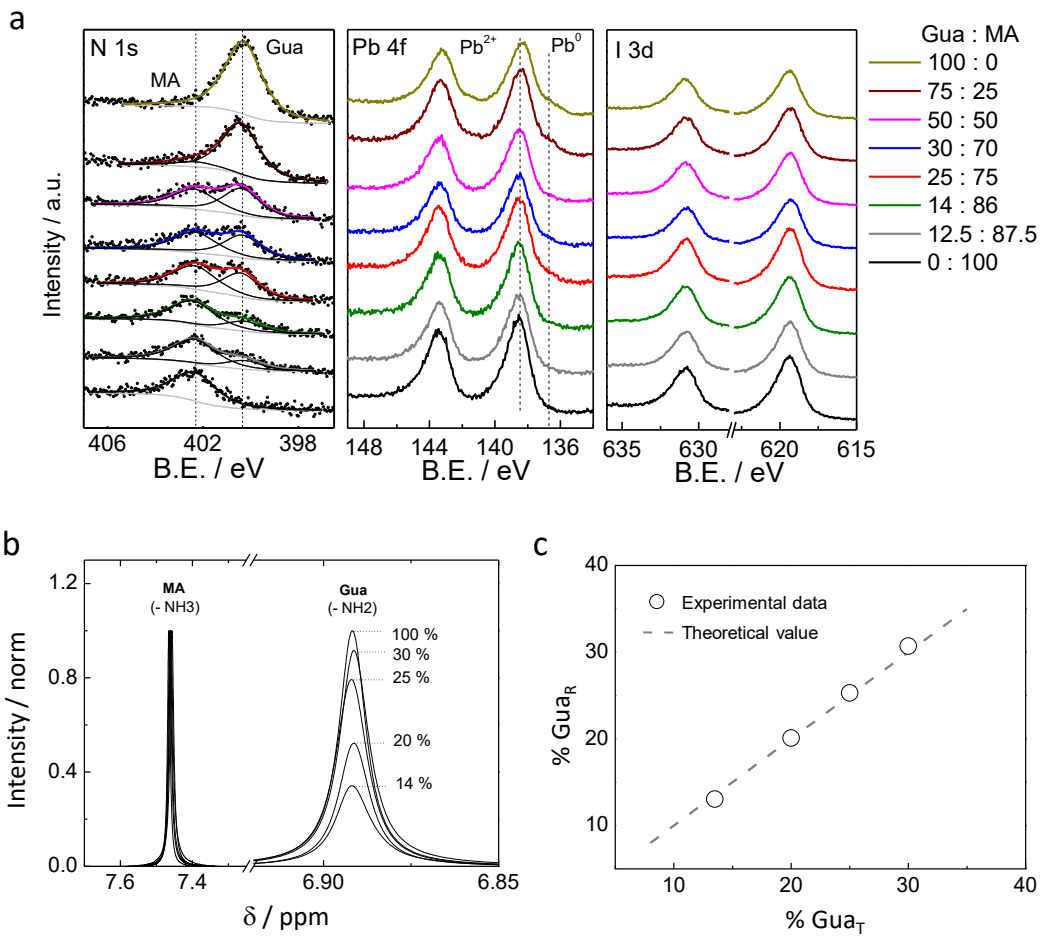

Supplementary Figure 2. a. XPS spectra of N 1s (left), Pb 4f (center) and I 3d (right) core level photoemission peaks[1] obtained from thin films of $MAPbI_3$ and mixed $MA_{1-x}Gua_xPbI_3$ systems (with x = 0.125, 0.25, 0.50, and 1.0). Traces have been shifted vertically for clarity. **b**, Liquid ^{1}H-NMR spectra obtained from $MA_{1-x}Gua_xPbI_3$ perovskite samples dissolved in d-DMSO, containing x = 0.14; 0.20; 0.25 and 0.30 (as indicated in the label). The relative ratio for $-NH_3$ and NH_2 groups (corresponding to MA and Gua respectively) is gradually decreasing with the increased incorporation of Gua. **c**, Quantification of MA:Gua ratio obtained from the ^{1}H-NMR spectra shown in (c) (Gua_R, value calculated from NMR spectra; Gua_T, theoretical value initially incorporated to the precursor solutions).

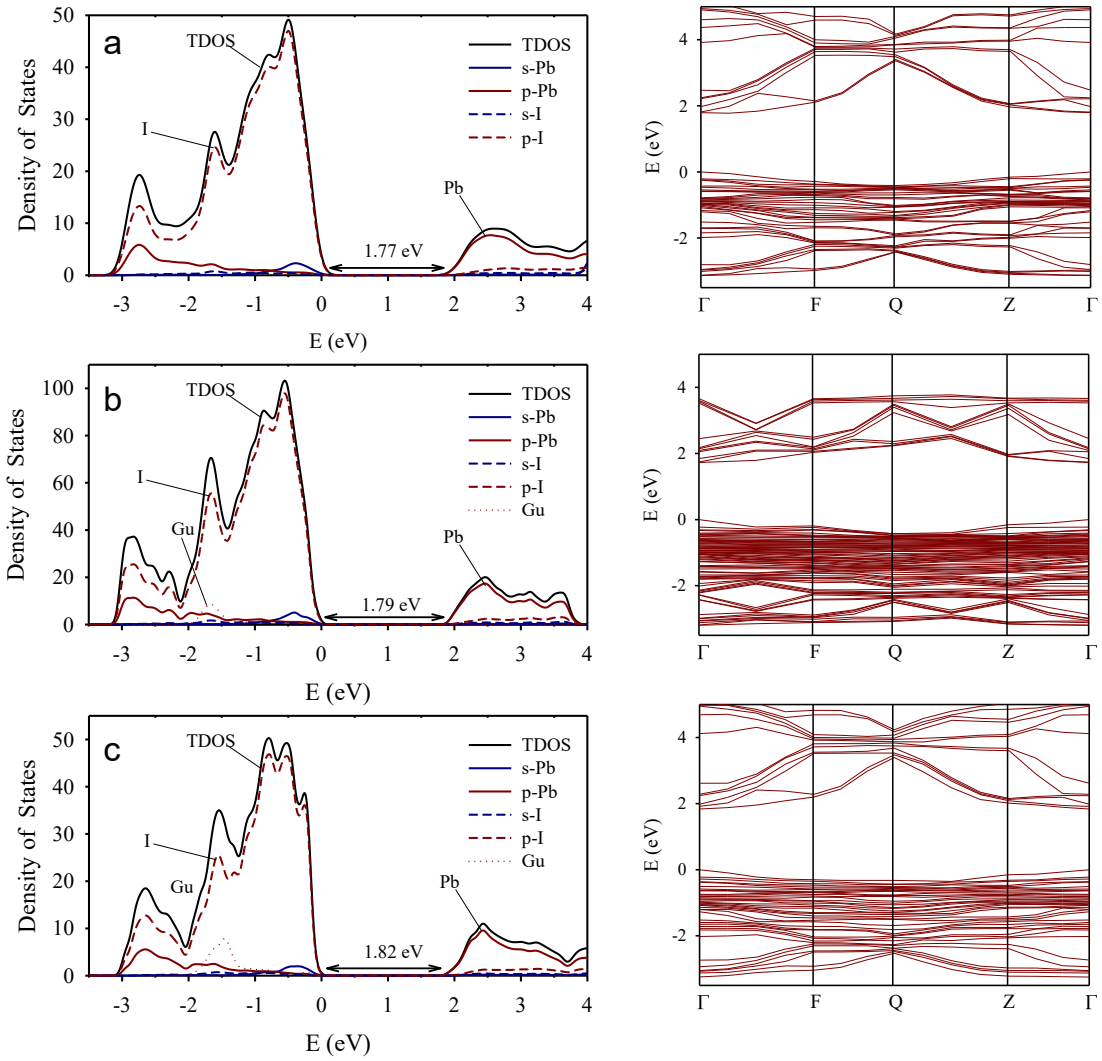

Supplementary Figure 3. Calculated band structure *(left)* and density of states *(right)* of **a**, $MAPbI_3$; **b**, $MA_{0.875}Gua_{0.125}PbI_3$ and **c**, $MA_{0.75}Gua_{0.25}PbI_3$. Inset: total (solid black line), s-Pb (blue solid line), p-Pb (red solid line), s-I (blue dashed line), p-I (red dashed line) and p-Gua (red dotted line) density of states.

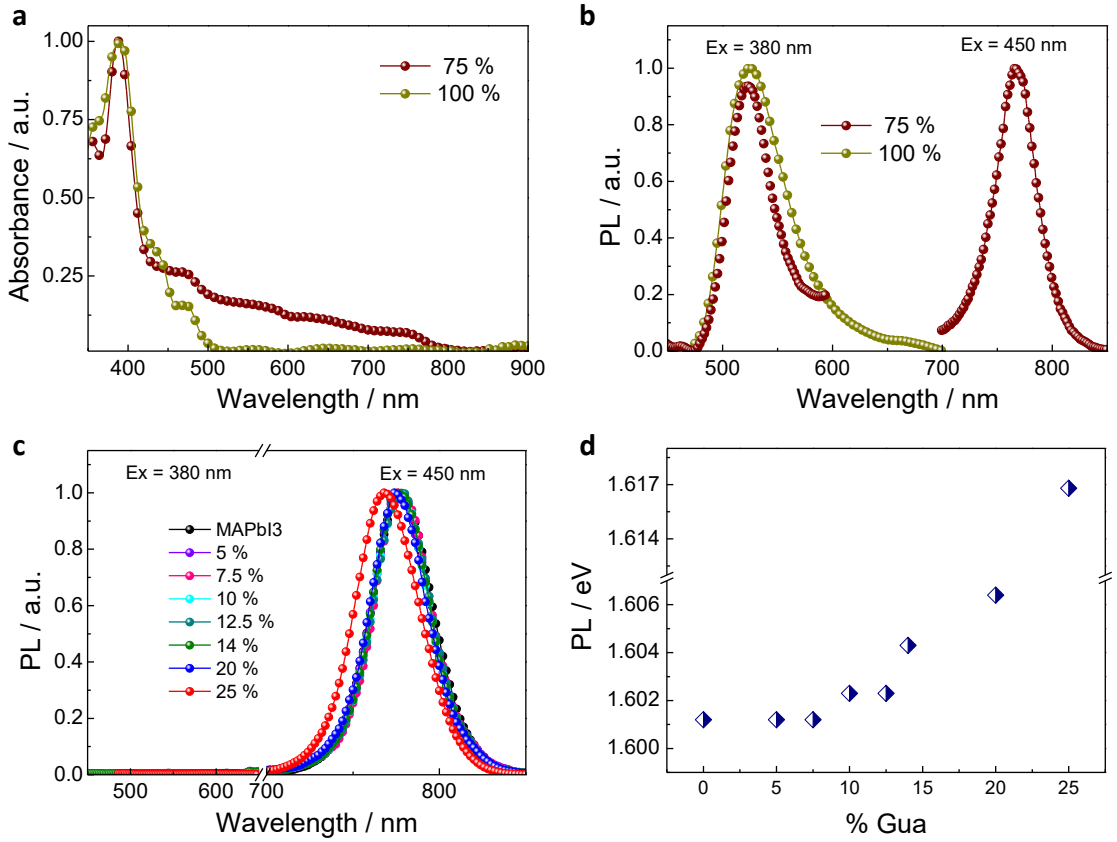

Supplementary Figure 4. a, UV-visible absorption spectra registered for MA:Gua mixed perovskite containing 75 % of Gua, as well as the pure 1D-GuaPbI$_3$ perovskite. **b**, Photoluminescence (PL) spectra registered for the systems presented in (a), excited at 380 nm (region below 700 nm) and 450 nm. The 75% sample exhibits emissions corresponding to the two coexisting phases (1D-GuaPbI$_3$, and MA$_{1-x}$Gua$_x$PbI$_3$). **c**, Photoluminescence (PL) spectra registered for MA$_{1-x}$Gua$_x$PbI$_3$ mixed perovskites containing $x \leq 0.25$, excited at both 380 nm (region below 700nm) and 450 nm. **d**, Evolution of the PL maximum (in eV) with % of Gua.

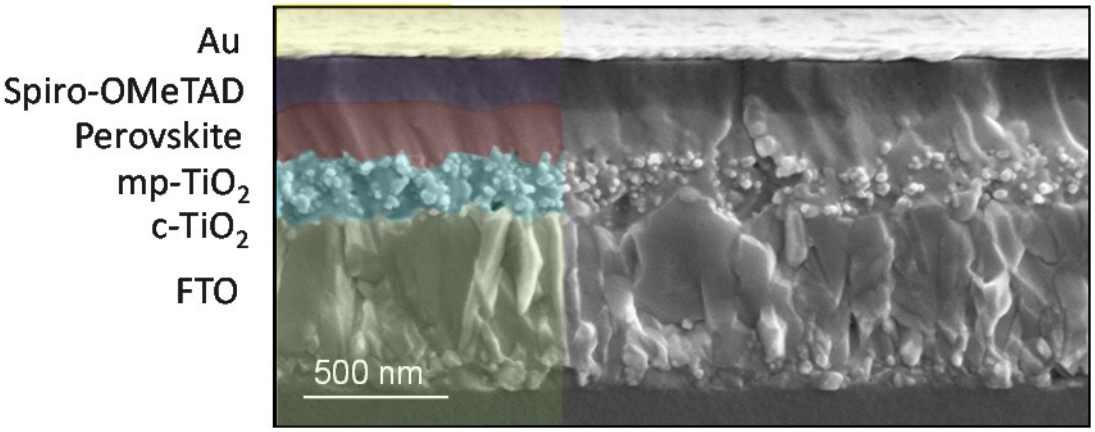

Supplementary Figure 5. Cross-sectional SEM image of a typical mixed MA:Gua PSC containing 14 % of Gua. Device architecture: Glass/FTO/c-TiO_2/ mp-TiO_2/ Perovskite/ Spiro-OMeTAD/ Au.

Supplementary Figure 6. Photographs of the MA:Gua mixed perovskite devices containing increased % of Gua, as indicated in the labels.

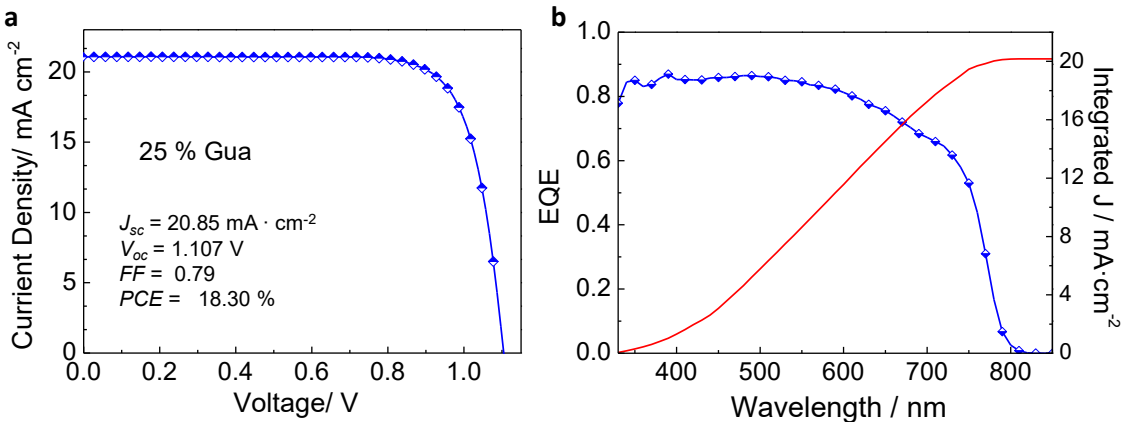

Supplementary Figure 7. Photovoltaic parameters obtained for the record cell containing $MA_{1-x}Gua_xPbI_3$ (x=0.25). **a**, Current density versus voltage ($J-V$) curve measured under AM1.5G sun illumination, at room temperature. **b**, *EQE* spectrum and integrated current density curve obtained for $MA_{1-x}Gua_xPbI_3$ solar cell (x=0.25).

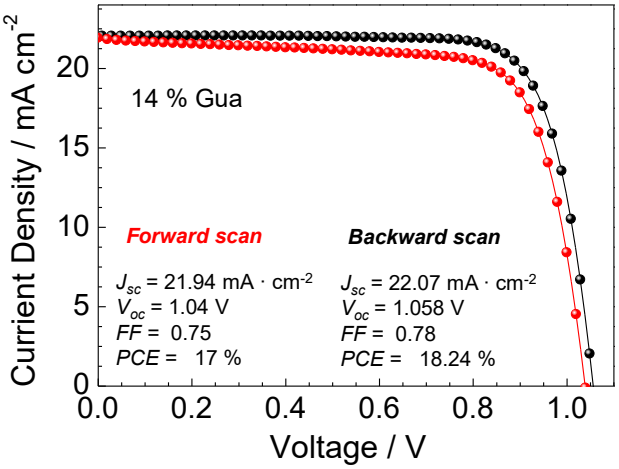

Supplementary Figure 8. $J-V$ curve measured for $MA_{1-x}Gua_xPbI_3$ (x=0.14) perovskite solar cell under forward (*Voc* to *Jsc*) and reverse (*Jsc* to *Voc*) bias conditions at AM1.5G sun illumination.

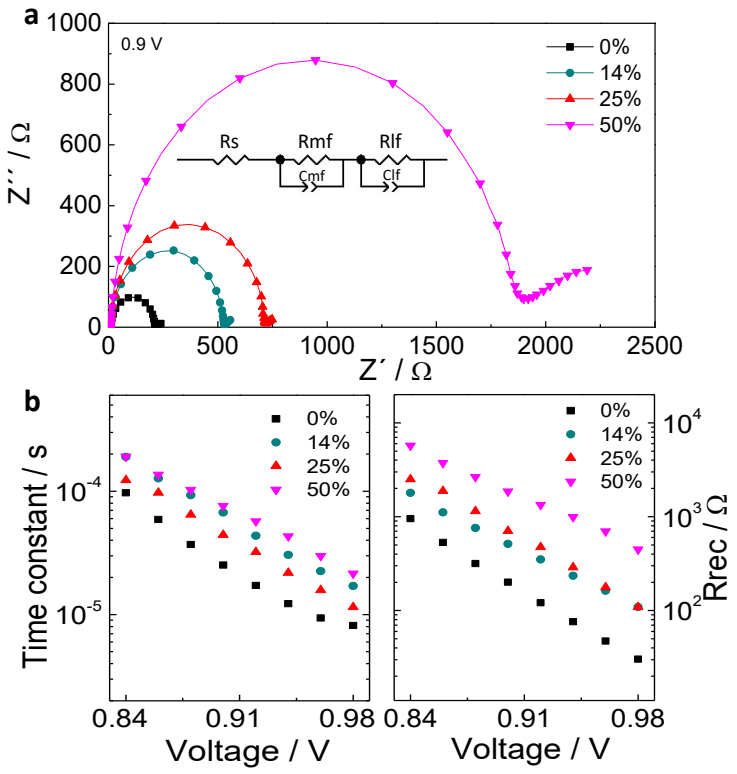

Supplementary Figure 9. a, Nyquist plot of PSCs prepared with MA:Gua systems containing increasing Gua content, as indicated in the label (the photovoltaic performance is presented in Supplementary Table 2). The equivalent circuit, shown in the inset, contains the series resistance (*Rs*), recombination resistance (*Rmf*, *Rlf*) and capacitance (*Cmf*, *Clf*) at medium and low frequency. **b**, Recombination resistance at medium frequencies (*Rmf*) versus applied voltage for the PSC analyzed in (a), *left panel*, and charge recombination time-constant calculated for perovskite devices shown in (a), *right panel*. See Supplementary Note 2.

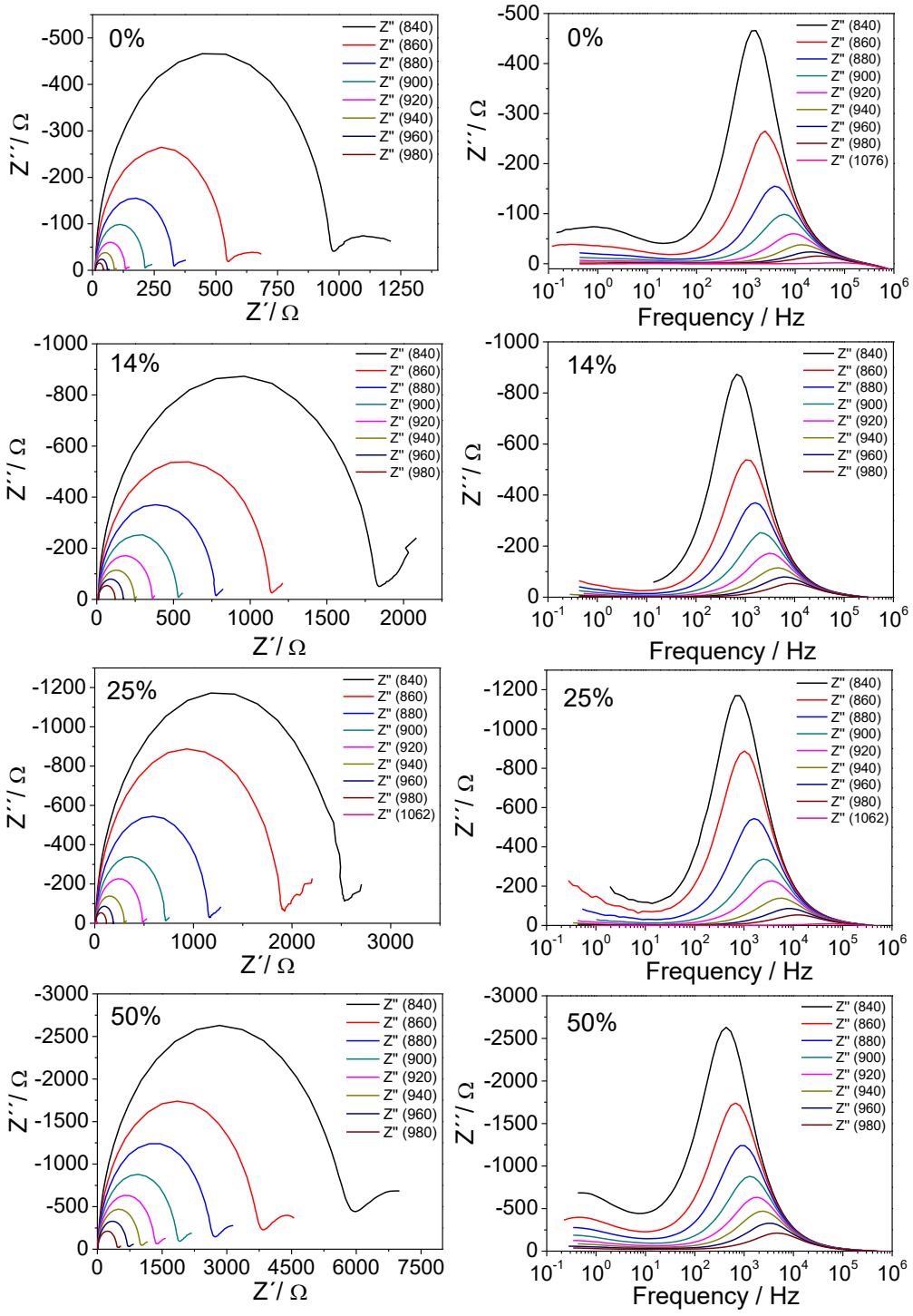

Supplementary Figure 10. Frequency plot of the imaginary part of the impedance response corresponding to the cells shown in Supplementary Table 2.

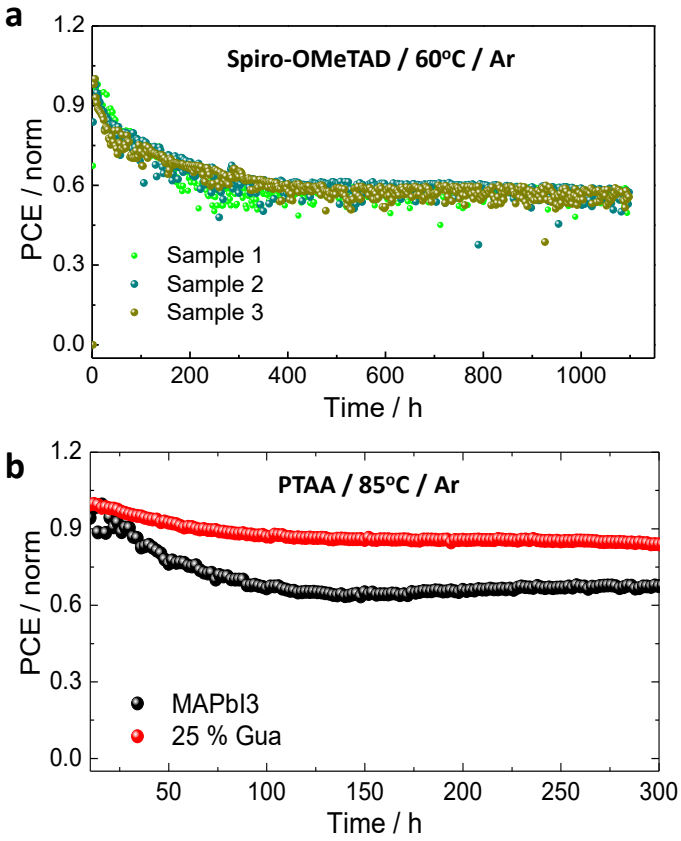

Supplementary Figure 11. Thermal stability test performed at maximum power point tracking (MPPT) under continuous light illumination of **a,** three different $MA_{1-x}Gua_xPbI_3$ (x = 0.125) perovskite solar cells containing Spiro-OMeTAD as HTM. Measurements performed at 60 ºC. **b**, $MA_{1-x}Gua_xPbI_3$ (x = 0.25) perovskite solar cell containing PTAA as HTM, $MAPbI_3$ is included as reference. Measurements performed at 85 ºC.

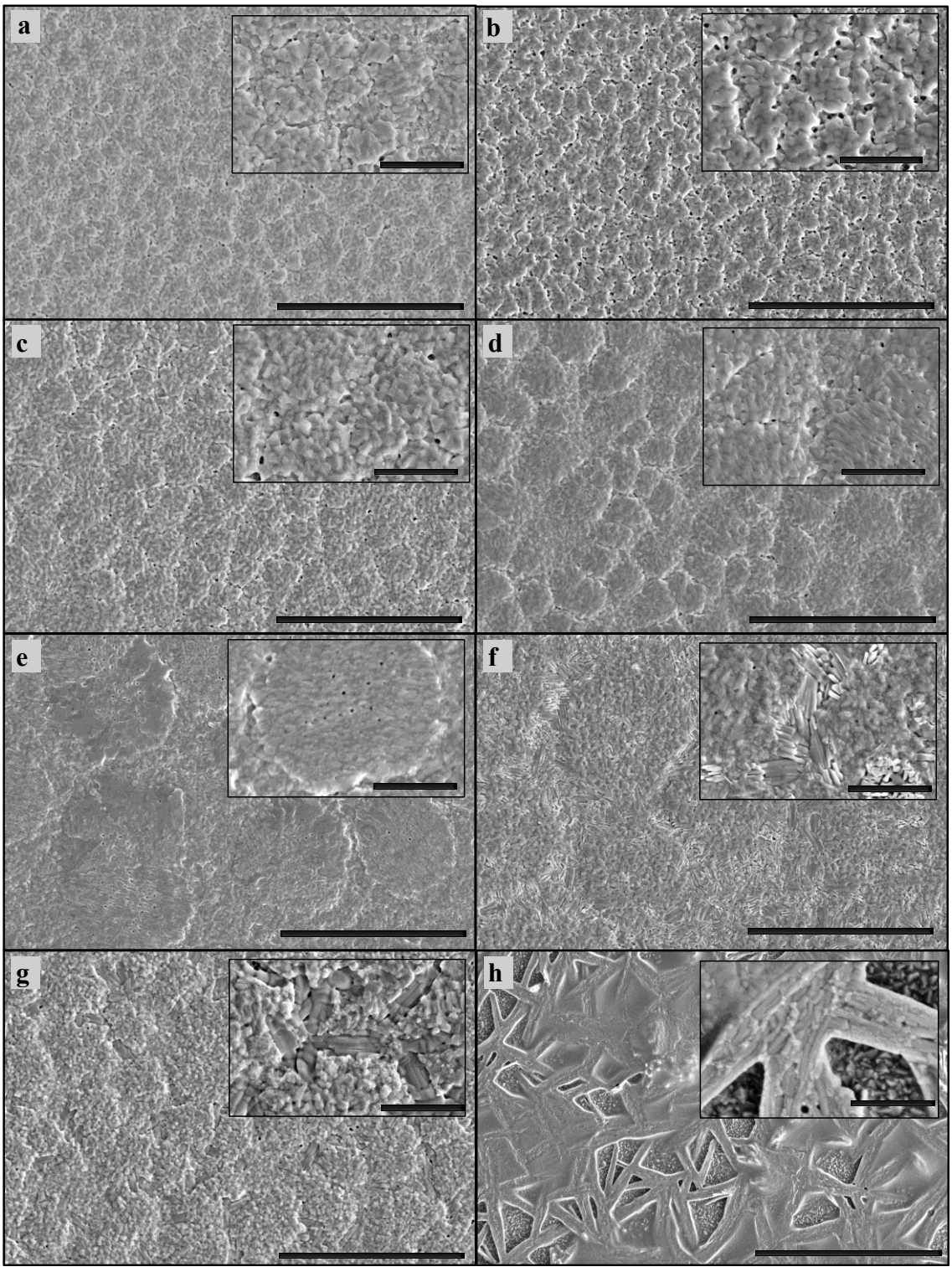

Supplementary Figure 12. Top view SEM images of a MA:Gua mixed systems at two different magnifications. The percentage of Gua incorporated into the system is (a) 0% ($MAPbI_3$), (b) 2.5 %, (c) 5 %, (d) 15 %, (e) 25 %, (f) 30 %, (g) 50 % and (h) 75 %. Large scale bar: 10 µm. Short scale bar *(inset)*: 2 µm.

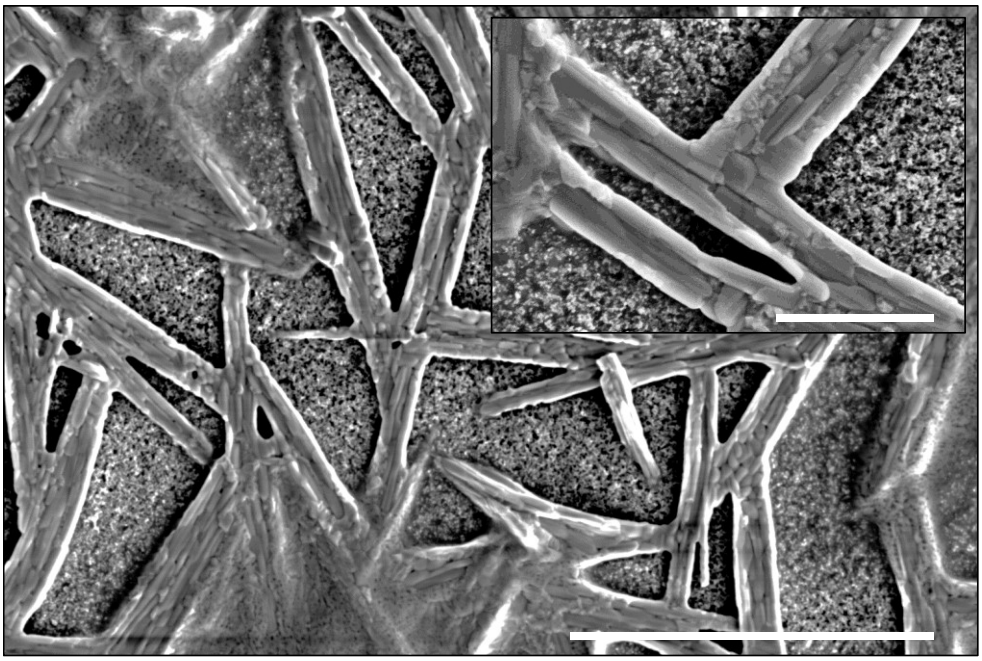

Supplementary Figure 13. Top view SEM image of a pure 1D-GuaPbI$_3$ perovskite sample on mp-TiO$_2$ substrate. Large scale bar: 10 µm. Short scale bar *(inset)*: 2 µm.

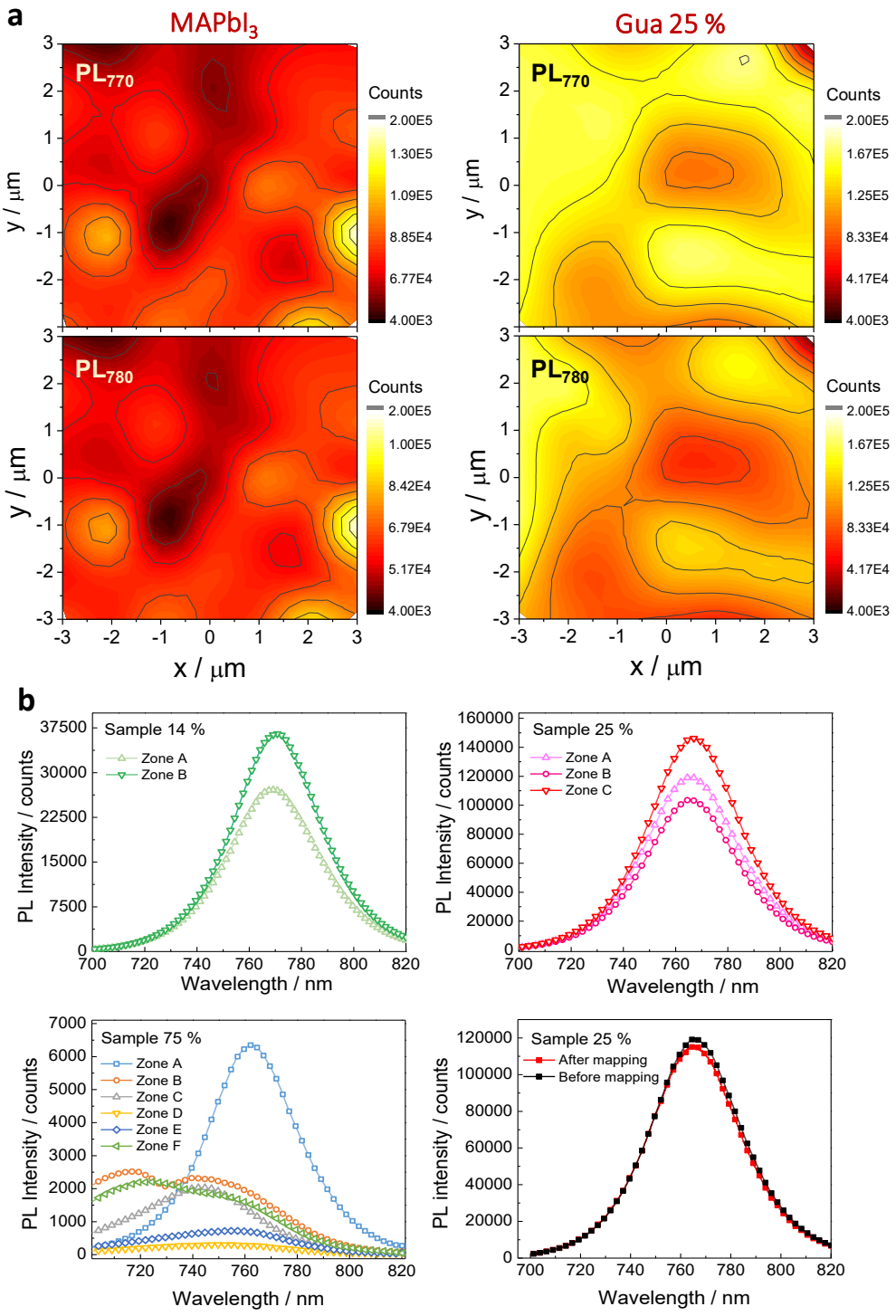

Supplementary Figure 14. a, Micro-PL intensity map of the perovskite surface obtained for $MAPbI_3$ and 25% Gua content (PL_{max} of 770nm (top) and 780nm (bottom)). The scalebar indicates the PL peak intensity in counts. **b**, PL emission peaks obtain from different zones in mixed $MA_{1-x}Gua_xPbI_3$ films (x = 0, 0.14 and 0.25). For comparison, the PL spectrum before and after the mapping has been recorded.

Supplementary Tables

Supplementary Table 1. Photovoltaic parameters obtained for the best performing cells containing MA:Gua perovskite systems measured under AM1.5G sun illumination. In brackets are indicated the averaged values for each condition from more than 190 devices (scan rate: 0.01 $V \cdot s^{-1}$; stabilization time: 5 s).

% Gua	J_{sc} *(mA·cm^{-2})*	V_{oc} *(V)*	*FF*	*PCE (%)*
0	22.50 (22.0 ± 0.8)	1.050 (1.04 ± 0.02)	0.80 (0.74 ± 0.04)	18.88 (17 ± 1)
2.50	22.28 (21.99 ± 0.7)	1.060 (1.058 ± 0.009)	0.76 (0.75 ± 0.04)	18.14 (17 ± 1)
5.00	22.49 (22 ± 1)	1.070 (1.054 ± 0.01)	0.782 (0.76 ± 0.02)	18.81 (17 ± 1)
7.50	22.49 (22.0 ± 0.4)	1.061 (1.05 ± 0.01)	0.786 (0.77 ± 0.03)	18.75 (17.8 ± 0.9)
10.0	22.53 (22.3 ± 0.3)	1.090 (1.07 ± 0.02)	0.777 (0.75 ± 0.03)	19.09 (17.8 ± 0.9)
12.5	22.79 (22.4 ± 0.5)	1.094 (1.07 ± 0.02)	0.785 (0.77 ± 0.03)	19.58 (18.3 ± 0.7)
14.0	23.19 (22.8 ± 0.3)	1.082 (1.07 ± 0.01)	0.803 (0.79 ± 0.01)	20.15 (19.2 ± 0.4)
15.0	22.34 (22.3 ± 0.4)	1.070 (1.07 ± 0.01)	0.795 (0.77 ± 0.02)	18.99 (18.4 ± 0.4)
17.0	22.54 (21.7 ± 0.5)	1.091 (1.08 ± 0.02)	0.785 (0.78 ± 0.02)	19.29 (18.1 ± 0.7)
20.0	21.31 (21.3 ± 0.5)	1.095 (1.08 ± 0.01)	0.790 (0.77 ± 0.03)	18.43 (17.7 ± 0.8)
25.0	20.85 (20.6 ± 0.7)	1.107 (1.09 ± 0.02)	0.790 (0.77 ± 0.02)	18.30 (17.1 ± 0.8)
50.0	12.79 (11 ± 2)	1.080 (1.09 ± 0.03)	0.667 (0.66 ± 0.02)	9.21 (8 ± 1)
75.0	0.59 (0.56 ± 0.08)	0.920 (0.88 ± 0.04)	0.600 (0.61 ± 0.04)	0.33 (0.30 ± 0.04)
100	0.50 (0.3 ± 0.3)	0.857 (0.882 ± 1)	0.394 (0.42 ± 0.04)	0.17 (0.12 ± 0.08)

Supplementary Table 2. Photovoltaic parameters measured for the four different samples employed for electro-chemical impedance spectroscopy (EIS) characterization.

Gua %	V_{oc} **(V)**	J_{sc} **(mA·cm^{-2})**	**FF**	**PCE (%)**
0	1.06	22.56	0.77	18.41
14	1.09	22.79	0.78	19.45
25	1.11	20.94	0.77	17.89
50	1.13	11.56	0.70	9.20

Supplementary Notes

Supplementary Note 1. To evaluate the stability of the proposed mixed $MA_{1-x}Gua_xPbI_3$ structures, the formation enthalpies, ΔH_f, of the pure MA or Gua perovskite phases and that containing 25% Gua were theoretically estimated by means of periodic DFT-GGA calculations using the PBE exchange correlation functional. To estimate the ΔH_f for each perovskite, we used the total energy per solid unit corresponding to each chemical specie depicted in eq. (1), which are obtained from the DFT-GGA calculations. The obtained values are a good approximation to the ΔH_f at zero temperature despite the zero-point vibrational energy and, less importantly, the standard pressure effects on the total energy are not considered[2]. Since the entropy contribution can be neglected at room temperature, ΔH_f can be utilized as a criterion for the stability of the different perovskites.

$$PbI_2 + (1-x)MAI + xGuaI \longrightarrow Ma_{1-x}Gu_xPbI_3 \qquad \text{eq. (1)}$$

The estimated formation enthalpies for the three studied materials are the following: for the $MAPbI_3$ material it is close to zero, -0.149 eV, which is very similar to that reported in a recent article (ΔH_f = -0.1 eV) by using similar DFT calculations[3]. Direct calorimetric measurements of ΔH_f have also revealed a positive value of 0.36 eV for $MAPbI_3$ [4]. Thus, both experimental and theoretical values of ΔH_f indicate the low stability of the $MAPbI_3$ perovskite with the chemical equilibrium in eq. (1) shifted to the initial precursors. This is clearly the origin of the poor stability of the solar cells prepared with this material. In the case of the 1D-$GuaPbI_3$ perovskite, the estimated value of ΔH_f is -2.045 eV, which indicates that eq. (1) is highly exothermic implying a great stability of the perovskite product [5]. Regarding the mixture with 25% Gua, $Ma_{0.75}Gua_{0.25}PbI_3$, the calculated ΔH_f is -1.484 eV, a highly negative value close to that of the 1D $GuaPbI_3$. The more negative value of ΔH_f in $Ma_{0.75}Gua_{0.25}PbI_3$ with respect to the $MAPbI_3$ perovskite indicates that the mixed phase is thermodynamically more stable than the pure phase. In addition, the optimization of the crystalline structure reveals the formation of hydrogen bonding, which plays a key role in the structural stabilization, revealing close distances in between the H atoms of the Gua cations and the I atoms. Although an evaluation of the H-bonds formation requires a more extensive theoretical investigation, these preliminary results indicates that the increased number of H atoms in the Gua results in larger number of H-bonds, which may be the ultimate responsible for the extended stability of the mixed $Ma_{0.75}Gua_{0.25}PbI_3$ systems compared to the archetypal $MAPbI_3$ perovskite.

Finally, to demonstrate that the addition of 25% Gua instead of MA leads to the formation of the mixed $Ma_{0.75}Gua_{0.25}PbI_3$ perovskite (eq. (1)) and not to a phase separation with 75% $MAPbI_3$ and 25% $GuaPbI_3$ (eq. (2)), the ΔH_f for the latter reaction was calculated.

$$PbI_2 + 0.75MAI + 0.25GuI \longrightarrow 0.75MaPbI_3 + 0.25GuaPbI_3 \qquad \text{eq. (2)}$$

The ΔH_f value for the formation of both perovskites, $MAPbI_3$ and $GuaPbI_3$, is -0.622 eV, less negative than that of the mixed phase formation, -1.484 eV. Thus, the formation of the mixed $Ma_{0.75}Gua_{0.25}PbI_3$ is thermodynamically favored with respect to the phase separation, which supports our experimental XRD results.

Supplementary Note 2. Supplementary Figure 10 presents the complex impedance plot obtained for cells containing various Gua % under illumination. Two arcs with different characteristic frequencies can be distinguished: one on the low frequency region 0,1-10 Hz, usually related to slow processes such as ionic motion or charge accumulation at the interfaces [6-8], and one in the mid-frequency region, 10^2-10^5 Hz, related with the recombination kinetics within the cell, as shown in Supplementary Fig. 11. Gua based solar cells exhibit better recombination resistance (it increases over 100 mV) and larger electron lifetime recombination compared with the $MAPbI_3$ reference.

Supplementary References

1. Wagner, C. D.; Riggs, W. M.; Davis, L. E., Handbook of X-ray photoelectron spectroscopy. *Muilenberg, G.E., Ed. Minnesota (*1979).

2. Huang, J. *et al.* Sequential Introduction of Cations Deriving Large-Grain $Cs_xFA_{1-x}PbI_3$ Thin Film for Planar Hybrid Solar Cells: Insight into Phase-Segregation and Thermal-Healing Behavior. *Small* **13**, 1603225, (2016).

3. Buin, A *et al.* Halide-Dependent Electronic Structure of Organolead Perovskite Materials. *Chemistry of Materials* **27**, 4405-4412, (2015).

4. Nagabhushana, G. P.*et. al.* Direct calorimetric verification of thermodynamic instability of lead halide hybrid perovskites. *Proceedings of the National Academy of Sciences* **113**, 7717-7721, (2016).

5. Quan, L. N. *et al.* Ligand-Stabilized Reduced-Dimensionality Perovskites. *Journal of the American Chemical Society* **138**, 2649-2655, (2016).

6. Bisquert, J.*et al.* Theory of Impedance and Capacitance Spectroscopy of Solar Cells with Dielectric Relaxation, Drift-Diffusion Transport, and Recombination. *The Journal of Physical Chemistry C* **118**, 18983-18991, (2014).

7. Guillén, E. *et al.* Elucidating Transport-Recombination Mechanisms in Perovskite Solar Cells by Small-Perturbation Techniques. *The Journal of Physical Chemistry C* **118**, 22913-22922, (2014).

8. Xiao, Z. *et al.* Giant switchable photovoltaic effect in organometal trihalide perovskite devices. *Nature Materials* **14**, 193-198, (2015).